

## UPDATES TO CAMx PLUME-IN-GRID MODEL TO IMPROVE NO<sub>y</sub> CHEMICAL PROCESSING AND COMPUTATIONAL SPEED

Chris Emery\*, Bonyoung Koo, Tan Sakulyanontvittaya, Greg Yarwood  
ENVIRON International Corporation, Novato, CA, USA

### 1. INTRODUCTION

Photochemical modeling is a complex process involving many supporting models and sub-models to simulate the atmosphere. For example, the Plume-in-Grid (PiG) sub-model within the Comprehensive Air quality Model with extensions (CAMx) treats the physical and chemical evolution of point source plumes when they are too small to be resolved by a modeling grid. The Greatly Reduced Execution and Simplified Dynamics (GREASD) PiG option is particularly focused on plumes from large NO<sub>x</sub> (NO+NO<sub>2</sub>) sources in which chemistry is controlled by high concentrations of NO<sub>x</sub>.

This study improved the computational efficiency of GREASD PiG by replacing its use of full photochemical mechanisms (e.g., Carbon Bond or CB) with a condensed mechanism comprising a limited number of inorganic reactions that are applicable during early plume stages when high NO<sub>x</sub> concentrations suppress oxidant production. The new PiG chemistry approach improved both speed performance and computational stability. In addition, reducing nocturnal minima for certain turbulence parameters decreased puff growth rates, resulting in plume widths that better agree with *in situ* aircraft measurements. Puff size plays a critical role in chemically aging plume NO<sub>x</sub> and subsequent impacts to grid ozone. CAMx sensitivity tests were conducted to analyze the effects of the modifications relative to the unmodified version of the model.

### 2. PiG MECHANISM DEVELOPMENT

The new GREASD PiG chemical mechanism was developed using a box model to emulate puff growth, dilution of emissions, entrainment of ambient background, and gas-phase chemistry. The box model also emulated the PiG “incremental chemistry” method that solves plume chemistry as a perturbation to background

chemistry. Initial tests with CB05 revealed a growing imbalance in total oxidized nitrogen (NO<sub>y</sub>) with NO<sub>y</sub> increasing by up to 30% after 4 simulation hours at night (Figure 1, top). Lack of nitrogen conservation was traced to the incremental chemistry approach and specifically to interactions between puff and background NO<sub>y</sub> in reactions that depend non-linearly on NO<sub>2</sub>. Setting the ambient background NO<sub>y</sub> (including NO<sub>2</sub>) to zero eliminated nitrogen non-conservation problems (Figure 1, bottom). Disregarding background NO<sub>y</sub> is reasonable for the early stages of NO<sub>x</sub> plumes when plume concentrations are larger than ambient NO<sub>y</sub>.

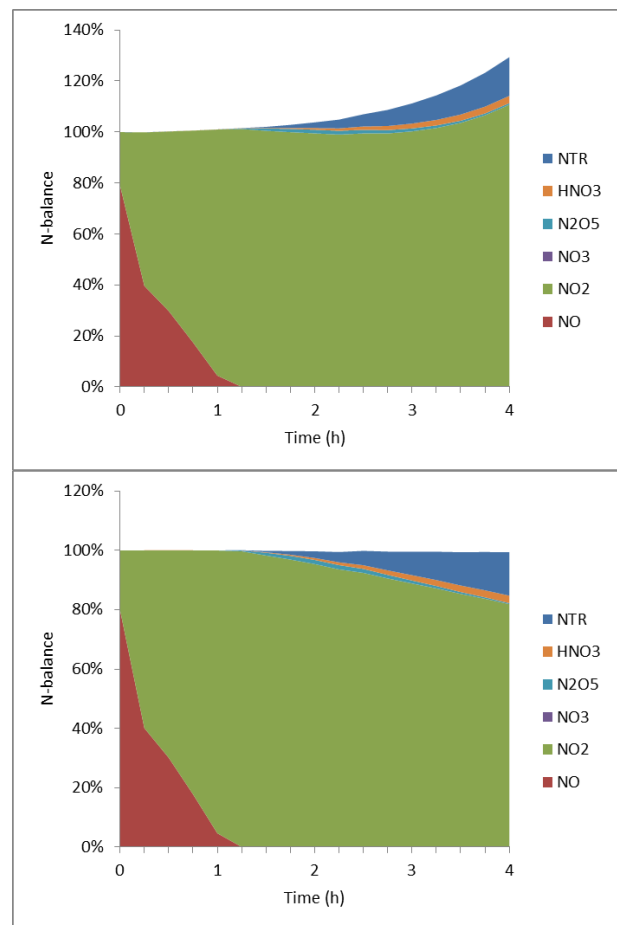


Fig. 1. Puff nitrogen balance for nighttime conditions with CB05 including background NO<sub>y</sub> contributions (top) and treating background NO<sub>y</sub> as zero (bottom).

\*Corresponding author: Chris Emery, ENVIRON International Corporation, Novato, CA 94998; e-mail: [cemery@environcorp.com](mailto:cemery@environcorp.com)

In CAMx, GREASD PiG now sets background NO<sub>y</sub> to zero while continuing to entrain background ozone as the main source of oxidants driving inorganic reactions.

The new mechanism for GREASD PiG includes 23 gas-phase reactions (Table 1) based on Karamchandani et al. (1998):

- Reactions for the NO-NO<sub>2</sub>-O<sub>3</sub> photo-stationary state established in sunlight (1-3);
- Self-reaction of NO important only at very high NO concentrations (4);
- Production of OH by photolysis of O<sub>3</sub> and HONO in sunlight (5-9);
- Production of nitric acid in sunlight (10);
- Formation of NO<sub>3</sub> and N<sub>2</sub>O<sub>5</sub> at night (11-17);
- Production of nitric acid at night (18);
- Production of sulfuric acid in sunlight (19);
- Removal of OH by CO (20);
- Production of OH by photolysis of formaldehyde (21-22);
- Conversion to OH of any HO<sub>2</sub> formed in 20-22 (23).

In-cloud aqueous conversion of SO<sub>2</sub> to sulfate and N<sub>2</sub>O<sub>5</sub> to nitric acid is also performed using the RADM mechanism (Chang et al., 1987).

Table 1. List of 23 reactions for GREASD PiG.

Number	Reaction
1	NO <sub>2</sub> = NO + O
2	O + O <sub>2</sub> + M = O <sub>3</sub> + M
3	O <sub>3</sub> + NO = NO <sub>2</sub>
4	NO + NO + O <sub>2</sub> = 2 NO <sub>2</sub>
5 <sup>1</sup>	NO + NO <sub>2</sub> + H <sub>2</sub> O = 2 HONO
6	O <sub>3</sub> = O <sub>1</sub> D
7	O <sub>1</sub> D + M = O + M
8	O <sub>1</sub> D + H <sub>2</sub> O = 2 OH
9	HONO = NO + OH
10	NO <sub>2</sub> + OH = HNO <sub>3</sub>
11	NO <sub>2</sub> + O <sub>3</sub> = NO <sub>3</sub>
12	NO <sub>3</sub> = NO <sub>2</sub> + O
13	NO <sub>3</sub> = NO
14	NO <sub>3</sub> + NO = 2 NO <sub>2</sub>
15	NO <sub>3</sub> + NO <sub>2</sub> = NO + NO <sub>2</sub>
16	NO <sub>3</sub> + NO <sub>2</sub> = N <sub>2</sub> O <sub>5</sub>
17	N <sub>2</sub> O <sub>5</sub> = NO <sub>3</sub> + NO <sub>2</sub>
18 <sup>2</sup>	N <sub>2</sub> O <sub>5</sub> + H <sub>2</sub> O = 2 HNO <sub>3</sub>
19	SO <sub>2</sub> + OH = SULF + HO <sub>2</sub>
20	OH + CO = HO <sub>2</sub>
21	FORM = 2 HO <sub>2</sub> + CO
22	FORM = CO
23	HO <sub>2</sub> + NO = OH + NO <sub>2</sub>

<sup>1</sup>Rate for GREASD PiG reaction 5 set to zero when used with SAPRC99.

<sup>2</sup>Rate for GREASD PiG reaction 18 may be enhanced by reaction on aerosol.

As part of this update, a new diagnostic criterion specific to the condensed mechanism was developed to define the crossover from a NO<sub>x</sub>-dominant regime to an oxidant production regime, at which point puffs transfer their mass to the grid regardless of puff size relative to the grid. The criterion is based on a radical chain length concept that determines the point at which radical propagation surpasses termination by NO<sub>2</sub>:

$$\frac{k_{OH}[SO_2] + k_{OH}[CO]}{k_{OH}[NO_2]} > 1. \quad (1)$$

The GREASD PiG mechanism can be run in tandem with any of the photochemical mechanisms used for grid chemistry (CB05, CB6 variants, or SAPRC99). Reaction rate constants and photolysis rates are taken directly from corresponding reactions in the grid chemical mechanism, which ensures consistency.

Box model tests showed good agreement for NO, NO<sub>2</sub> and O<sub>3</sub> concentrations between the condensed mechanism and CB05. Initial testing in CAMx with MPI and OMP parallelization confirmed correct implementation and measured efficiency improvements. In the regional modeling tests described below using OMP parallelization across 12 processors, the new PiG mechanism reduced computational time spent on PiG by 80-85% and reduced overall CAMx runtime by 25-30%.

### 3. RESULTS

CAMx/PiG testing was conducted using pre-existing CB05 modeling datasets covering the eastern US, which were developed by the Texas Commission on Environmental Quality (TCEQ) and the US Environmental Protection Agency (EPA). Initial tests focused on a single NO<sub>x</sub> plume from the Oklaunion power plant in north-central Texas on the night of October 10-11. Results were compared to data collected from aircraft flights traversing the plume (Yarwood et al., 2012). Testing with an EPA July 2005 dataset was performed to analyze daily impacts to simulated surface ozone, NO<sub>y</sub>, and SO<sub>x</sub> on regional scales.

#### 3.1 Testing Nocturnal Plumes

Figure 2 displays a snapshot at 10 PM on October 11 of the simulated plume emanating from Oklaunion and heading southward for roughly 2 hours, consistent with aircraft observations. Three different cases are overlaid: the plume as explicitly resolved on a super high-resolution

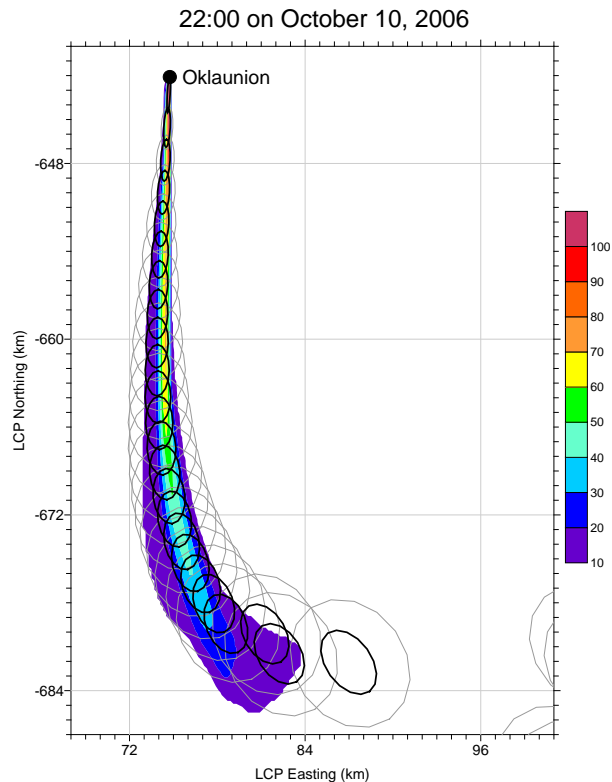


Fig. 2. Comparison of the train of CAMx PiG puff dimensions (ellipses) against the super-high resolution NO<sub>2</sub> plume (colored contours in ppb) in CAMx layer 5 at 10 PM on October 10, 2006. Grey puffs are those from the original v5.41 PiG, and the smaller black puffs are the result of reducing nighttime growth rates as described by ENVIRON (2012).

nested grid at 200 m resolution (color contours); a train of PiG puffs from the original PiG in CAMx version 5.41 (grey ellipses); and a train of PiG puffs from the new PiG (black ellipses). Puff widths are symmetrically defined as  $\pm 1.5\sigma$  about the puff centerline ( $3\sigma$  total width), where  $\sigma$  is one standard deviation of a Gaussian distribution.

The super high-resolution grid was employed by Yarwood et al. (2012) to explicitly simulate the evolution of the Oklaunion plume in lieu of the PiG model. The high resolution plume was consistently about 1 km wide within an hour of release and slowly grew to several km wide well downstream. This was in very good agreement with the aircraft transects.

Plume growth in the original PiG was quickest just after release and slowed after 30 minutes. The plume was consistently between 5 and 10 km wide out to 2 hours, which was wider than ~1 km widths observed in aircraft transects at similar distances downwind.

The new PiG case with reduced nighttime puff growth rates was much improved in matching the plume width from aircraft measurements and the explicit high-resolution run. Puff sizes grew slowly up to about 2 km after 1 hour of transport time and up to about 3 km after 2 hours. Vertical puff spread was well replicated and so vertical puff growth rates were not modified (Yarwood et al., 2012; ENVIRON, 2012).

Figure 3 compares the chemical evolution of the entire ~2 hour PiG puff streams shown in Figure 2 (10 PM) as incremental concentrations relative to grid background. Results from three PiG cases are shown, along with cross-plume average measurements from aircraft transects at about 14 and 30 km downwind of Oklaunion (roughly 35 and 80 minutes of modeled transport time, respectively). Transect averages are also expressed as incremental concentrations relative to background measurements well outside the plumes. We defined the plume widths for the calculation of transect averages according to the cross-section of measured NO concentrations clearly above background (>10 ppb). For both transects resulting plume widths were about 1 km.

Modeled NO<sub>x</sub> and ozone concentrations were identical between the original PiG and new chemistry cases, which indicates that the primary conversion of NO<sub>x</sub> along the plume is correctly modeled with the condensed mechanism. NO<sub>x</sub> in the reduced growth case remained more concentrated in the smaller puff volumes. Aircraft NO measurements indicate better agreement with the reduced growth case but this is not so clear for NO<sub>2</sub>. Ozone may be the likely cause of the discrepancy between observed and modeled NO<sub>2</sub>. Plume ozone deficits of 30 to 40 ppb are simulated in the various PiG cases, but only 20 ppb deficits were measured. Simulated background ozone was about 40 ppb while measured background was about 25 ppb, so in reality nearly half the ozone was available to convert NO directly to NO<sub>2</sub>. This explains the higher measured NO and lower NO<sub>2</sub> than simulated in the PiG even with reduced growth rates. Nevertheless, the reduced growth case extends higher NO<sub>x</sub> and negative ozone increments farther downwind in better agreement with measurements.

Turning to plume production of NO<sub>z</sub> (HNO<sub>3</sub> and N<sub>2</sub>O<sub>5</sub>), all three PiG cases vary. The original PiG allows for negative NO<sub>z</sub> increments as background contributions are involved in PiG chemistry. Both NO<sub>z</sub> components go negative in the original PiG case during the latter half of the first hour, but they remain at zero in the new chemistry case as designed. Aircraft

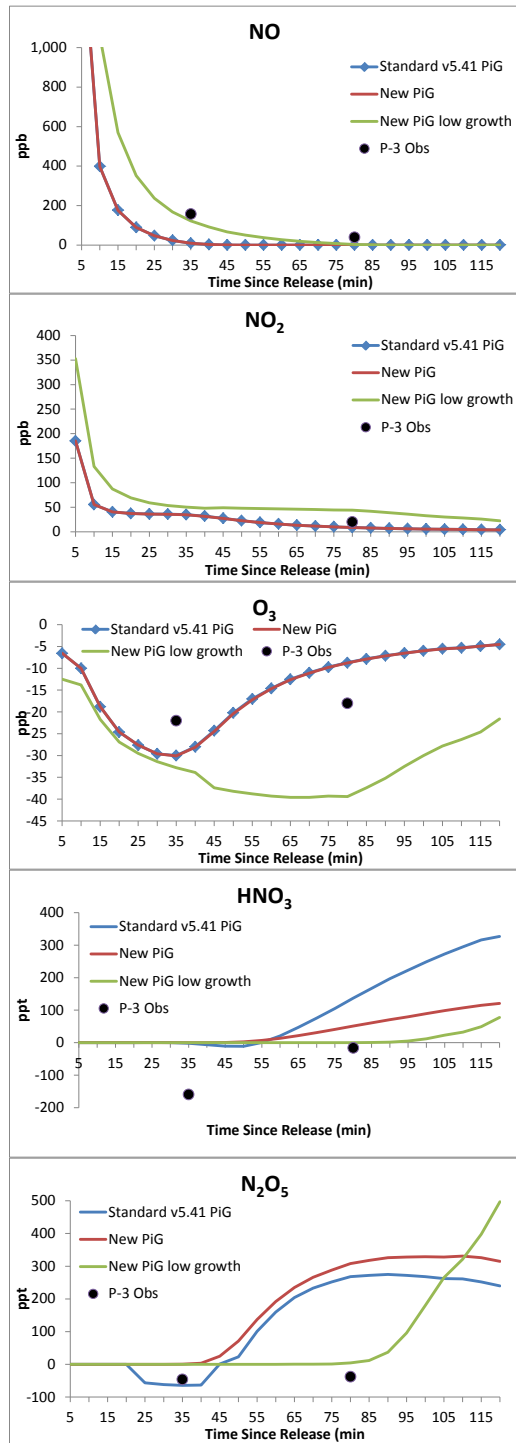


Fig. 3. Chemical evolution in the stream of puffs from Oklaunion at 10 PM on October 10, 2006. Results from three PiG simulations (colored lines) are compared to cross-plume averaged aircraft measurements at two transects (black dots). All simulated and measured concentrations are shown relative to ambient background.

measurements also show negative plume increments, especially for  $\text{HNO}_3$ , but this is more likely related to conversion to aerosol nitrate which is not treated by PiG. The production of  $\text{NO}_z$  increases in both the original PiG and new chemistry cases at about 1 hour downwind. The new chemistry case squelches  $\text{HNO}_3$  production but slightly increases  $\text{N}_2\text{O}_5$  production relative to the original PiG. The reduced growth case suspends  $\text{NO}_z$  production until late in the second hour. Aircraft measurements suggest no generation of plume  $\text{NO}_z$  at the two transects shown, which further supports limiting plume growth rates in these tests.

The condensed PiG chemical mechanism performed similarly to CB05. Reducing the nocturnal horizontal puff growth rates better matched the measured plume widths and the chemical conversion of  $\text{NO}_x$  to  $\text{NO}_z$ . Vertical puff spread was well replicated and so vertical puff growth rates were not modified.

### 3.2 Regional Response

CAMx was run for July 2005 on a 36 km grid covering North America. Figure 4 displays the ozone distribution on July 1 from a run without PiG, and differences in ozone at the same hour resulting from various PiG configurations.

The PiG treatment has historically resulted in relatively small isolated ozone impacts compared to no-PiG runs, and our results are consistent with this feature (Figure 4, top right). For obvious reasons the ozone impacts tend to be isolated to grid cells around large  $\text{NO}_x$  point sources, and are usually largest for coarser resolution. Ozone impacts tend to be smaller in higher-resolution (12 and 4 km) grids because puffs dump quickly due to size constraints and more of the plume chemistry is handled directly by the grid chemistry.

Implementation of the new PiG chemistry alone, i.e. without modifications to puff growth, does not change this behavior significantly (Figure 4, bottom left). However, there is a reduction in the number of grid cells where ozone is substantially reduced, and more areas of ozone increases. This may be related to improved nitrogen conservation, but is more likely caused by the revised chemical dumping criterion, which dramatically alters the behavior of the puff population over the day.

While detailed analyses show that reduced nighttime puff growth rates result in a better evolution of in-plume  $\text{NO}_y$  and ozone, we remain concerned with the lack of interaction between

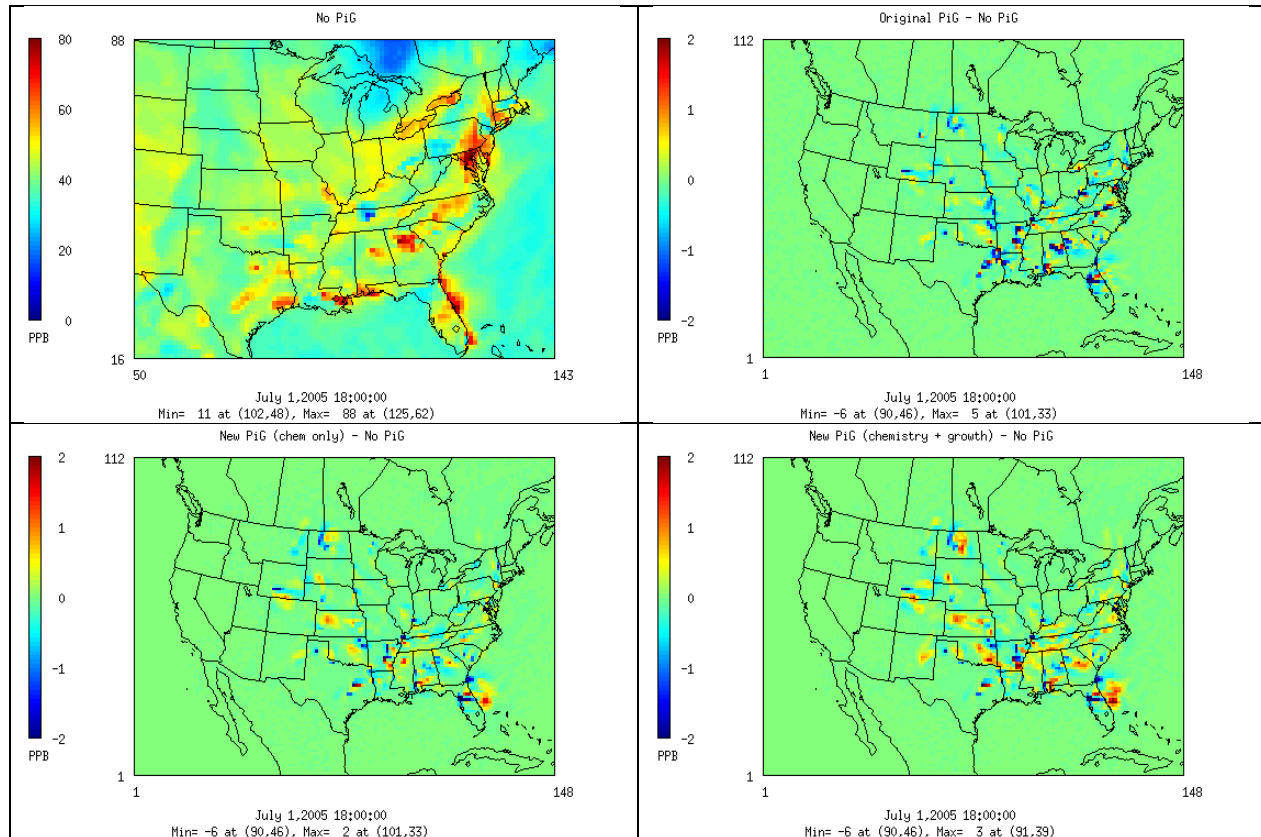


Fig. 4. Ozone responses to different PiG configurations on the 36 km grid at 18 UTC July 1, 2005. (Top left) Ozone distribution resulting from a run without PiG; (top right) ozone difference resulting from original PiG; (bottom left) ozone difference resulting from new PiG chemistry along; (bottom right) ozone difference resulting from new PiG chemistry and reduced nighttime puff growth rates.

puff-sequestered NO<sub>y</sub> and background NO<sub>y</sub> in the grid, especially for older, diluted, expansive puffs that cover significant fractions of coarse grid volumes. We introduced a new parameter to limit the maximum puff size and trigger dumping to the grid. Puffs are now terminated when they grow to grid scale (as in the original approach), or when they reach a new maximum size limit, whichever is smaller. We set the default size limit to 10 km based on the conceptual argument that the puff coherency assumption is increasingly invalid approaching and exceeding this scale.

The combined effects on ozone from new chemistry, reduced nighttime growth rates, and a new maximum puff size constraint are shown in Figure 4 (bottom right). Results are very similar to the chemistry-only modification but with some evidence of slightly higher positive ozone impacts. Reduced puff growth rates dramatically increased the number of puffs overnight by almost a factor of

two while extending average puff ages from about 2 hours to 6 hours. CAMx runtimes were only marginally impacted by a few percent.

While patterns of PiG vs. no-PiG differences in secondary inorganic products are consistent between the original and new PiG treatments, in this particular test the new PiG tended toward more NO<sub>z</sub> (expressed as nitric acid in Figure 5) and more sulfate than the original PiG. This is likely a combined result of the updated chemical dumping criterion and reduced puff growth rates, which extended chemical production of these secondary products for several additional hours. The effect is more pronounced for longer-lasting puffs traversing coarser grids (e.g., 36 km) and minimal for finer resolutions where puffs are terminated by size constraints well before meeting chemical constraints.

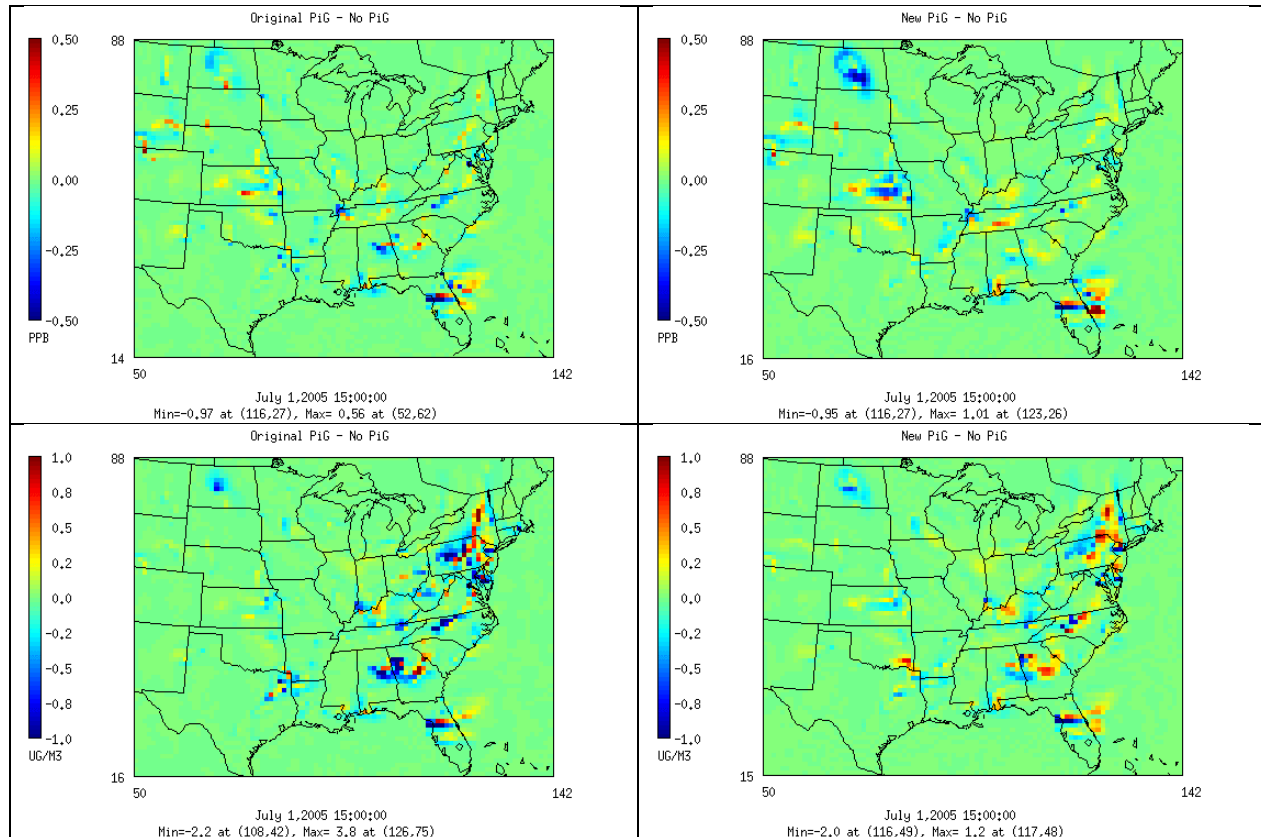


Fig. 5. Nitric acid (top row) and sulfate (bottom row) responses to different PiG configurations in the 36 km grid at 15 UTC on July 1, 2005. Differences between original PiG and no PiG runs are shown on the left, and differences between the new PiG (with updates to both chemistry and growth) and no PiG runs are shown on the right.

## 8. REFERENCES

- Chang, J.S., R.A. Brost, I.S.A. Isaksen, S. Madronich, P. Middleton, W.R. Stockwell, C.J. Walcek. 1987. A Three-dimensional Eulerian Acid Deposition Model: Physical Concepts and Formulation. *J. Geophys. Res.*, 92, 14,681-14,700.
- ENVIRON, 2012. "Dallas-Fort Worth modeling support: Improving vertical mixing, Plume-in-Grid, and photolysis rates in CAMx." Final report to the TCEQ, Work Order 582-11-10365-FY12-06 (August 2012).
- Karamchandani, P., A. Koo, C. Seigneur, 1998. "Reduced gas-phase kinetic mechanism for atmospheric plume chemistry." *Environ. Sci. Technol.*, 32, 1709-1720.
- Yarwood et al., 2012. "NO<sub>x</sub> reactions and transport in nighttime plumes and impacts on next-day ozone." Final report for the Texas Air Quality Research Program, Project 10-020 (January 31, 2012), [http://aqrp.ceer.utexas.edu/viewproject\\_s.cfm?Prop\\_Num=10-020](http://aqrp.ceer.utexas.edu/viewproject_s.cfm?Prop_Num=10-020).

## 9. ACKNOWLEDGMENT

We thank Doug Boyer at the Texas Commission on Environmental Quality (TCEQ) for helpful discussions on mechanism development, testing, and results. This work was sponsored by the TCEQ.